Study of the Kinetics and Mechanism of Rapid Self-Assembly in Block Copolymer Thin Films during Solvo-Microwave Annealing

ARTICLE *in* LANGMUIR · AUGUST 2014

Impact Factor: 4.46 · DOI: 10.1021/la503137q · Source: PubMed

7 AUTHORS, INCLUDING:

Sozaraj Rasappa
Technical University of Denmark
30 PUBLICATIONS **165** CITATIONS
SEE PROFILE

Claudia C. D. Simao
Eurecat
27 PUBLICATIONS **184** CITATIONS
SEE PROFILE

Clivia M. Sotomayor Torres
Catalan Institute of Nanoscience and Nanotec…
485 PUBLICATIONS **6,242** CITATIONS
SEE PROFILE

Michael A Morris
Trinity College Dublin
353 PUBLICATIONS **4,867** CITATIONS
SEE PROFILE

Langmuir

Article

pubs.acs.org/Langmuir

Study of the Kinetics and Mechanism of Rapid Self-Assembly in Block Copolymer Thin Films during Solvo-Microwave Annealing

Parvaneh Mokarian-Tabari,*[,†,‡] Cian Cummins,[†] Sozaraj Rasappa,[†,‡] Claudia Simao,[§] Clivia M. Sotomayor Torres,[§,∥] Justin D. Holmes,[†,‡] and Michael A. Morris[†,‡]

[†]Department of Chemistry, University College Cork and Tyndall National Institute, Cork, Ireland

[‡]Centre for Research on Adaptive Nanostructures and Nanodevices (CRANN) and AMBER Centre, Trinity College Dublin, Dublin, Ireland

[§]Catalan Institute of Nanoscience and Nanotechnology ICN2, Campus de la UAB, Barcelona 08193, Spain

[∥]Catalan Institute for Research and Advanced Studies (ICREA), Barcelona 08010, Spain

ABSTRACT: Microwave annealing is an emerging technique for achieving ordered patterns of block copolymer films on substrates. Little is understood about the mechanisms of microphase separation during the microwave annealing process and how it promotes the microphase separation of the blocks. Here, we use controlled power microwave irradiation in the presence of tetrahydrofuran (THF) solvent, to achieve lateral microphase separation in high-χ lamellar-forming poly(styrene-*b*-lactic acid) PS-*b*-PLA. A highly ordered line pattern was formed within seconds on silicon, germanium and silicon on insulator (SOI) substrates. *In-situ* temperature measurement of the silicon substrate coupled to condition changes during "solvo-microwave" annealing allowed understanding of the processes to be attained. Our results suggest that the substrate has little effect on the ordering process and is essentially microwave transparent but rather, it is direct heating of the polar THF molecules that causes microphase separation. It is postulated that the rapid interaction of THF with microwaves and the resultant temperature increase to 55 °C within seconds causes an increase of the vapor pressure of the solvent from 19.8 to 70 kPa. This enriched vapor environment increases the plasticity of both PS and PLA chains and leads to the fast self-assembly kinetics. Comparing the patterns formed on silicon, germanium and silicon on insulator (SOI) and also an *in situ* temperature measurement of silicon in the oven confirms the significance of the solvent over the role of substrate heating during "solvo-microwave" annealing. Besides the short annealing time which has technological importance, the coherence length is on a micron scale and dewetting is not observed after annealing. The etched pattern (PLA was removed by an Ar/O_2 reactive ion etch) was transferred to the underlying silicon substrate fabricating sub-20 nm silicon nanowires over large areas demonstrating that the morphology is consistent both across and through the film.

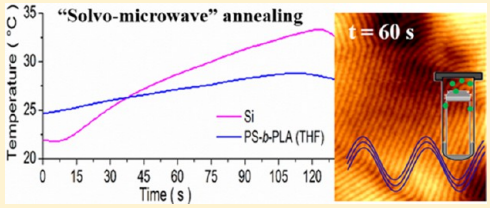

INTRODUCTION

Self-assembled block copolymer (BCP) thin films are a potential candidate for the fabrication of nanofeatures such as nanopillars, nanowires, and nanowells beyond the capacity of current photolithography techniques. However, long annealing times,[1] the lack of a defect-free long-range-order pattern, and a complex lift-off and etch process[2,3] are some of the obstacles that need to be addressed for the successful implementation of this technique in advanced patterning. Some of these issues can be improved by using a more strongly segregated or "high-χ" block copolymer since as χ increases one can move to lower molecular weights while maintaining the thermodynamic driving force for low defectivity small feature size, and increasing chemical contrast for improved etching or selected material inclusion.

Annealing times (since BCP systems do not usually spontaneously form long-range-ordered patterns at room temperature) are critical as pattern quality is determined by the ability of a BCP to eliminate defects such as dislocations by chain motion.[4] While in general morphological improvement is provided by higher χ BCPs, it also reduces the kinetics of polymer diffusion during thermal annealing.[5] With regard to thin films, molecules are restricted in their motions due to confinement effects. In lamellar-forming block copolymers, the layered structure imposes additional constraints on the mobility and diffusion of the chains,[6] which is an important factor in defect annihilation. The diffusion in perpendicular lamellar BCPs can happen along the domains (parallel diffusion), but the elimination of defects requires "hopping diffusion" which requires a chain to diffuse perpendicular to the interface.[5] This involves a chain breaking away from the interface and relocating at the opposite interface. The diffusion across a domain involves mixing within the domain. For high-χ BCPs, the increased penalty of mixing results in a slower diffusion rate and higher kinetic barriers and subsequently leads to significantly longer annealing times.[4−7]

Received: May 20, 2014
Revised: August 19, 2014
Published: August 19, 2014

   dx.doi.org/10.1021/la503137q | *Langmuir* 2014, 30, 10728−10739

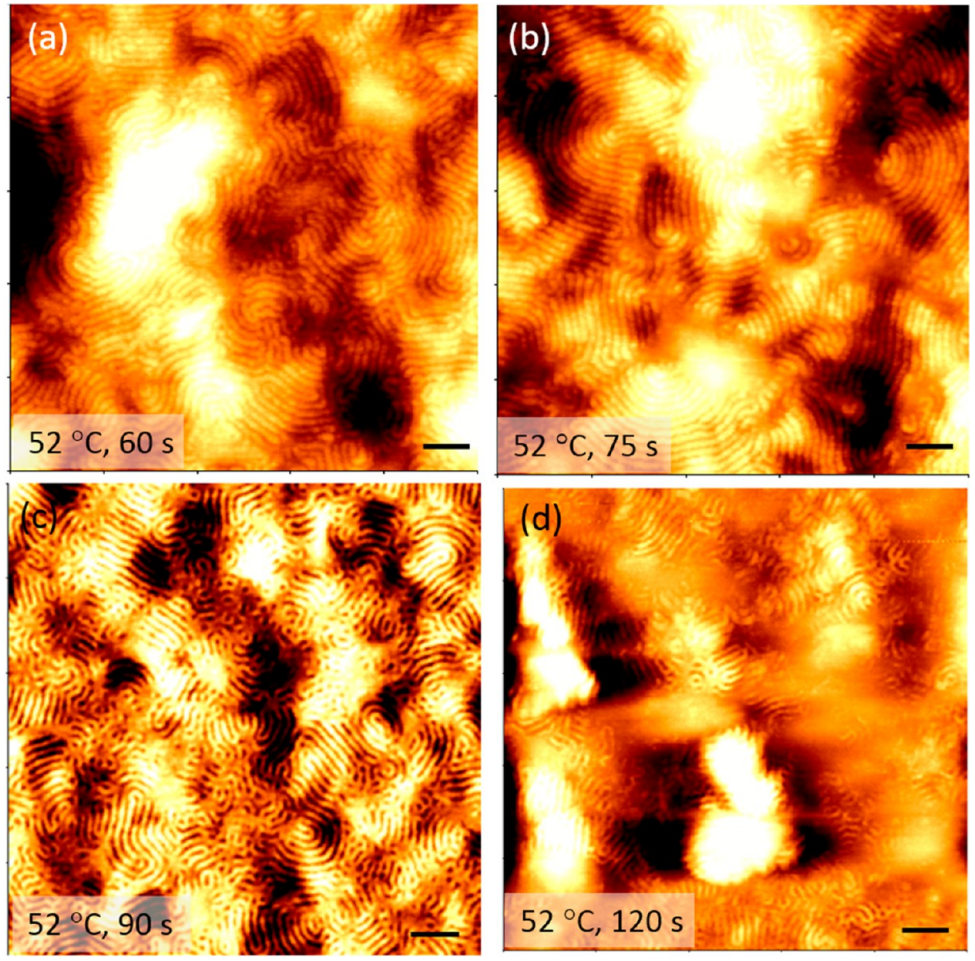

Figure 1. AFM topographic images showing poor microphase separation of PS-*b*-PLA at 52 °C without surface modification. (a) After 60 s, (b) after 75 s, (c) after 90 s, and (d) after 120 s of solvo-microwave annealing. The film dewets at longer times. The scale bars are 200 nm.

Microwave-assisted microphase separation appears to offer considerable advantages in reducing annealing times in a number of BCP systems, and we show that we can overcome long annealing times associated with a relatively high χ poly(styrene-*b*-lactic acid) (PS-*b*-PLA) (χ = 0.217 at 25 °C)[8] system by utilizing microwave energy. Microwave annealing was first demonstrated by Zhang and Buriak.[9,10] So far, it has been employed for annealing commonly used poly(styrene-*b*-methyl methacrylate) (PS-*b*-PMMA)[9,11,12] and poly(styrene)-*b*-poly(2-vinylpyridine) (PS-*b*-P2VP)[10,9,12] block copolymers. Recently, the use of microwaves has been demonstrated with a poly(styrene-*b*-dimethylsiloxane) (PS-*b*-PDMS) system with and without solvent.[11,13] Microwave annealing has also been used to make a dispersion of poly(styrene-*b*-isoprene) PS-*b*-PI nanoparticles in water.[14] However, despite the promise of this technique, little is known about the mechanism of how microwave irradiation might sponsor the molecular motion that accompanies microphase separation. Buriak and coworkers have championed substrate heating as the primary source of molecular motion driven by defects in silicon substrates that absorb microwave radiation.[12] However, recent results within our group seem to indicate this may not be the case in all systems and we suggest that microwave absorption by the solvent molecules might also make a significant contribution to the annealing process. We have modified the system to carefully monitor temperature and extended the substrate range to amplify our model, and this is reported here. Our results are quantified through defect analysis software that we have developed for BCP thin film metrology.[15]

The PS-*b*-PLA system is of particular interest. PLA is a biodegradable aliphatic polyester and can be chemically etched to provide an on-chip etch mask for pattern transfer.[16−18] In hexagonal-forming PS-*b*-PLA, the thermal annealing process can be very long (12 h) and problematic due to the thermal degradation of PLA.[17,19] Solvent vapor annealing has recently been shown for PS-*b*-PLA and seems more practical.[16,20] Recent reports have examined lamellar-forming PS-*b*-PLA systems.[21−24] Depending on the difference in the surface energy of the substrate/air with each block or the confinement effect, the lamellae can align either perpendicular or parallel to the substrate.[25] To achieve perpendicular alignment, a surface-modification step is generally required, which is usually done by applying a SAM (self-assembled monolayer), a brush layer, or chemical patterning of the substrate.[26,27] Surface modification can be complicated and requires prolonged treatment periods. Previously, we have reported the perpendicular alignment of lamellar PS-*b*-PEO systems through a stepwise thermo/solvent annealing system without any surface modification.[28,29] Here, we describe a simple and yet very fast technique for perpendicular alignment of the domains in lamellar PS-*b*-PLA diblock copolymer using a microwave unit in the presence of appropriate solvents, which leads to formation of highly ordered patterns within 45 s. To understand the interaction of polymers with microwave irradiation, we carried out an in

dx.doi.org/10.1021/la503137q | *Langmuir* 2014, 30, 10728−10739

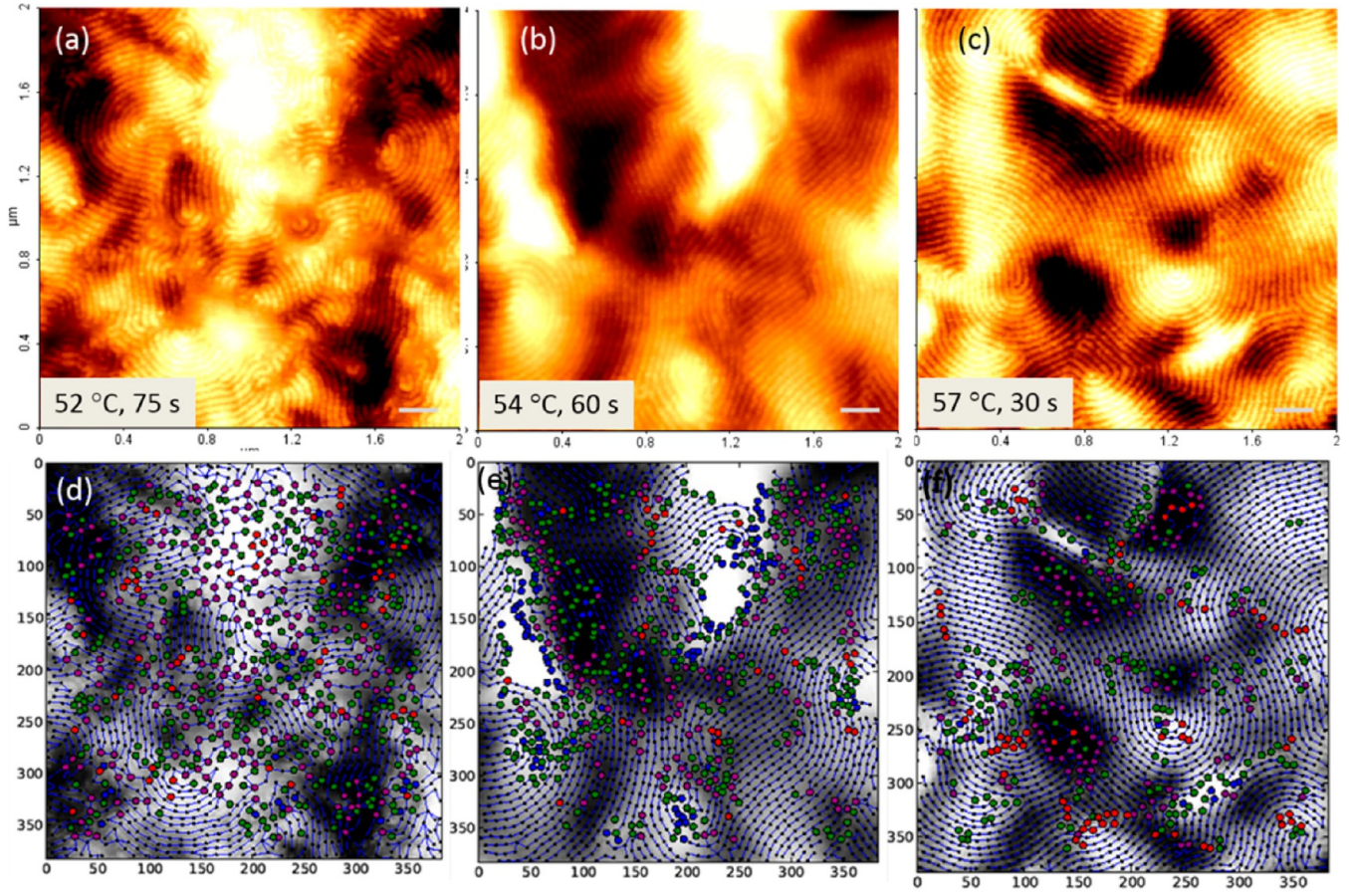

Figure 2. Higher impact of temperature over microwave annealing time on the ordering of the PS-*b*-PLA film. Higher temperature and lower annealing time (c) provide a better degree of order than low temperature and longer annealing time (a, b). The scale bars are 200 nm. (d–f) Line element (dark-blue dashed dots) and defect identification (color coding: end points (green), lone points (blue), branch points (purple). and turn points (red) related to images a–c.

situ temperature measurement of the substrate during the annealing. This provided further insight into the microwave-related process. This was followed by a reactive ion etch (RIE) step to remove PLA. We have measured the etch selectivity of PS and PLA in a controlled way by manipulating the DC bias indirectly. The remaining template was pattern transferred to the silicon substrate using an RIE-ICP (inductively coupled plasma) etcher, which led to the fabrication of well-ordered 16 nm silicon nanowires.

EXPERIMENTAL SECTION

Materials. Lamellar-forming (PS-*b*-PLA) block copolymer was purchased from Polymer Source with number-average molecular weights of $M_{n,PS}$ = 21 kg mol^{-1} and $M_{n,PLA}$ = 19.5 kg mol^{-1}, f_{PS} = 0.55, and PDI = 1.06. The block copolymer was used without any further modifications. Thin films of PS-*b*-PLA films were spun cast from 2 wt % chloroform solution onto silicon substrates.

Substrate Preparation. The silicon substrates were sonicated in different solvents such as ethanol, acetone, and isopropanol. However, they all result in poor microphase separation under solvo-microwave annealing. The best results were achieved when samples were exposed to UV/ozone for 45 min prior to spin-casting.

Solvo-Microwave Annealing and in Situ Temperature Measurement. Figure 4 shows the industrial microwave unit we used to process the samples. In Figure 4b, the microwave vial is displayed. The temperature is controlled at the bottom of the vial with an infrared (IR) probe. We used two smaller glass vials to raise the level of the solvent and also to provide a support base to hold the substrate. The power was set at 300 W, and a range of temperatures were tested. However, as the temperature range in our experiments was not too high (50–60 °C), in practice only a small amount of power (less than 50 W) was applied to reach the set temperature. A range of thermal and solvent annealing steps in tetrahydrofuran, toluene, water, chloroform, acetone, and mixtures thereof were tested up to 70 °C in the microwave.

Etch and Pattern Transfer. To measure the etch rate of PS and PLA, the homopolymers of PS and PLA with number-average molecular weights of $M_{n,PS}$ = 16 kg mol^{-1} (PDI = 1.03) and $M_{n,PLA}$ = 16 kg mol^{-1} (PDI = 1.30) were etched at the same time with PS-*b*-PLA films. The dry etch was performed in an Oxford Instruments Plasmatech in RIE (reactive ion etching) mode using a mixture of argon (15 sccm) and O_2 (10 sccm) at a processing pressure of 12 mTorr, an rf power of 40 W, and a dc bias of 145 V. More details regarding the etch parameters for the PS-*b*-PLA film can be found elsewhere.[30] The remaining PS mask was pattern transferred to a silicon substrate using a combination of sulfur hexafluoride (SF_6) and trifluoromethane (CHF_3) gases in an STS AOE inductively coupled plasma (ICP) etcher.[3] The residual PS stripes after the pattern transfer were removed by O_2 plasma.

Film Characterization. Atomic force microscopy (AFM) (Park Systems, XE-100) was operated in ac (tapping) mode under ambient conditions using silicon microcantilever probe tips with a force constant of 42 N m^{-1}. Topographic and phase images were recorded simultaneously. Scanning electron microscopy (SEM) images were obtained by a FEI Helios Nanolab 600i system at an accelerating voltage of 5 kV and at a working distance of 4 mm. Cross-section SEM images involved cleaving the substrate in half and positioning the substrate perpendicular to the incident beam of electrons. The stage was then tilted at 20°. To achieve a contrast between PS and PLA in

dx.doi.org/10.1021/la503137q | *Langmuir* 2014, 30, 10728–10739

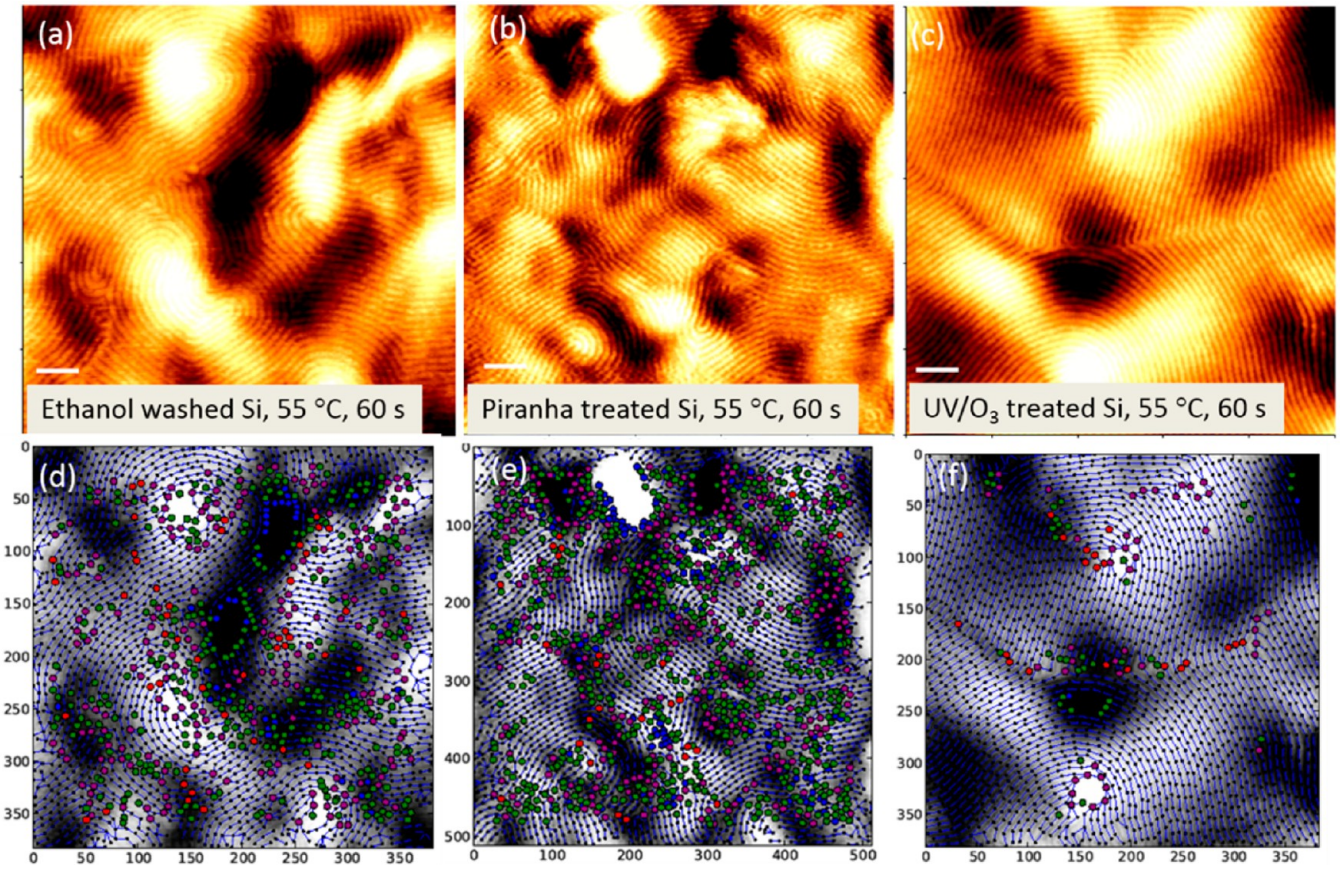

Figure 3. Effect of UV/ozone on the long-range order of PS-*b*-PLA thin films. The samples were solvo-microwave annealed at 55 °C for 60 s. The silicon substrate was (a) sonicated in ethanol for 10 min, (b) cleaned in piranha solution, and (c) exposed to UV/ozone for 45 min. The UV/ozone surface treatment provides the best long-range order. The pitch is 34 nm. The scale bars are 200 nm. (d–f) Correlated defect analysis. The (UV/ozone)-treated substrate has the lowest defect density (f) and the highest average line length. See Figure 9 for more details.

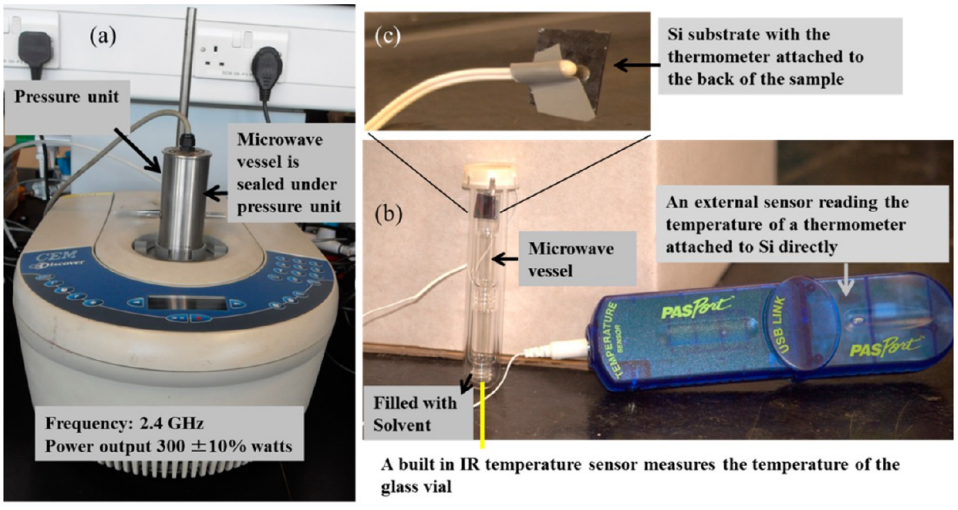

Figure 4. 2.4 GHz microwave unit. The pressure vessel (a) seals the microwave glass vessel shown in (b). The smaller glass vials in (b) are to hold the sample above the solvent level. A built-in IR sensor measures the temperature at the bottom of the glass vial. (c) An external thermometer is attached to the silicon substrate and to a sensor (PASPort TM). That sensor is linked to a laptop via a USB cable and reads the temperature of the silicon continuously during microwave annealing.

SEM, the PS domains were stained by ruthenium tetroxide (RuO_4).[31] A solution of ruthenium tetroxide was prepared by mixing ruthenium trichloride hydrate (Sigma) with active chlorine aqueous sodium hypochlorite (Sigma). Ruthenium trichloride hydrate (0.1 g) was weighed out, and in a fume hood 5 mL of 13% active chlorine aqueous sodium hypochlorite was slowly added. This was then placed in a small desiccator with the cleaved film as seen in fig6Figure 8d to selectively stain PS domains with RuO_4 vapors and provide contrast for SEM characterization. Note that caution should be taken when using RuO_4, and organic solvents should not come into contact with the substance.

Defect Analysis. To estimate the defect density in the images, we have used our recently developed defect analysis software.[15] The code

dx.doi.org/10.1021/la503137q | *Langmuir* 2014, 30, 10728–10739

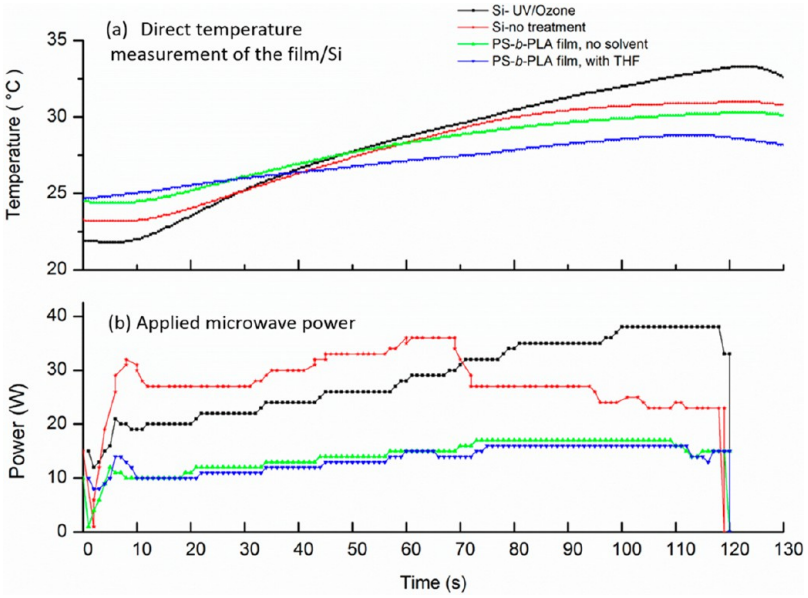

Figure 5. In situ temperature measurement during exposure to microwave radiation. (a) Direct temperature measurement of the silicon substrate and PS-*b*-PLA film by a thermometer attached to the back of the substrate and the film (b) applied microwave power range for different sets of experiments shown in (a). The temperature of the silicon substrate and the PS-*b*-PLA did not exceed the set value of 55 °C at any time during annealing. Color code (a, b): black squares, (UV/ozone)-treated Si; red stars, Si substrate with no treatment; green triangles, PS-*b*-PLA film on Si with no solvent; and blue triangles, PS-*b*-PLA film with THF in the annealing vial.

has been developed to identify lines and defects specifically from block copolymer self-assembly. After the region of interest is chosen in the image, the first computational step identifies the elements (lines) and four types of DSA defects (lone or break points, branching, dislocation, and turning points). The defects are color-coded for illustration. The colored dots are then overlaid with the original AFM or SEM image and the marked lines, as seen in Figure 2. The defect density is then estimated as follows:

$$\text{defect density} = \frac{\text{no. branching} + \text{no. turning} + \text{no. lone} + \text{no. end}}{\text{area}} \quad (1)$$

The collected statistics concerning the identification and quantification of the defects is summarized in Figure 9. More details about the software and defect types can be found in ref 15.

RESULTS AND DISCUSSION

Effect of Temperature and Time on Solvo-Microwave Annealing. Microwave annealing is a new recognized way of heating selected substrates rapidly and affecting microphase separation in a short period of time.[10] Here we outline a new dynamic effect where substrates remain "cool" and microphase separation is brought about through the "activation" of polar solvent molecules as discussed in detail below. It should be initially pointed out that controlling and measuring the temperature during short microwave annealing periods is challenging as the power is varied (as in this setup) or pulsed to effectively vary the temperature. During the user-defined temperature ramp, the power and hence temperature can fluctuate considerably. This causes some irregularity in results; therefore, care must be taken. Moreover, the IR probe measures the temperature at the bottom of the microwave vessel rather than the silicon substrate (Figure 4b). We tried different temperatures from 40 to 60 °C in the presence of different solvents and without solvent. In the absence of solvent and with microwave annealing only, no microphase separation was attained in PS-*b*-PLA films at temperatures below 60 °C.

The 200-nm-thick PS-*b*-PLA films were exposed to THF at different temperatures during solvo-microwave annealing. A nominal power of 300 W, a ramp time of 5 min (unless otherwise stated), and an irradiation time of 30−180s was applied. Note that here the practical applied power was much less than 300 W. For example, it was around 30 W for an annealing temperature of 55 °C. 50 °C was observed as the minimum temperature needed to observe microphase separation even in the presence of THF. This is consistent with the known glass-transition temperature (T_g) of PLA in our PS-*b*-PLA system (49 °C), suggesting that solvent swelling significantly reduces T_g in the crystalline phase. Increasing the temperature from 52 to 57 °C improves the order in PS-*b*-PLA thin films. However, we will discuss later that the actual temperature of the silicon substrate and the polymer film is lower than the set temperature of 55 °C and perhaps the fast increase in the vapor pressure of THF, a polar solvent, plays a more significant role in suppressing the glass transition of the film and improving the order.

The AFM topographic image in Figure 1 shows the results at an annealing temperature of 52 °C. A poorly ordered microphase-separated pattern is observed after 60 s (Figure 1a), and increasing the time does not improve the long-range order noticeably (Figure 1b). Note that it was not possible to maintain stable temperatures at annealing periods shorter than 60 s for temperatures of less than about 55 °C.

The annealing temperature has a greater influence on enhancing the coherence length of the pattern in comparison to the annealing time. As shown is Figure 2, annealing at 57 °C for 30 s (Figure 2c) induces a better ordering rearrangement than annealing at 52 °C for 75 s or at 54 °C for 60 s (Figure 2a,b). Figure 2d−f shows the defect analysis software output of the line element (dark-blue dashed dots) and the color-coded defect identification related to Figure 2a−c. The statistical defect analysis of the samples is summarized in Figure 9 for all images. As seen in Figure 9a, the average line length in Figure

dx.doi.org/10.1021/la503137q | *Langmuir* 2014, 30, 10728−10739

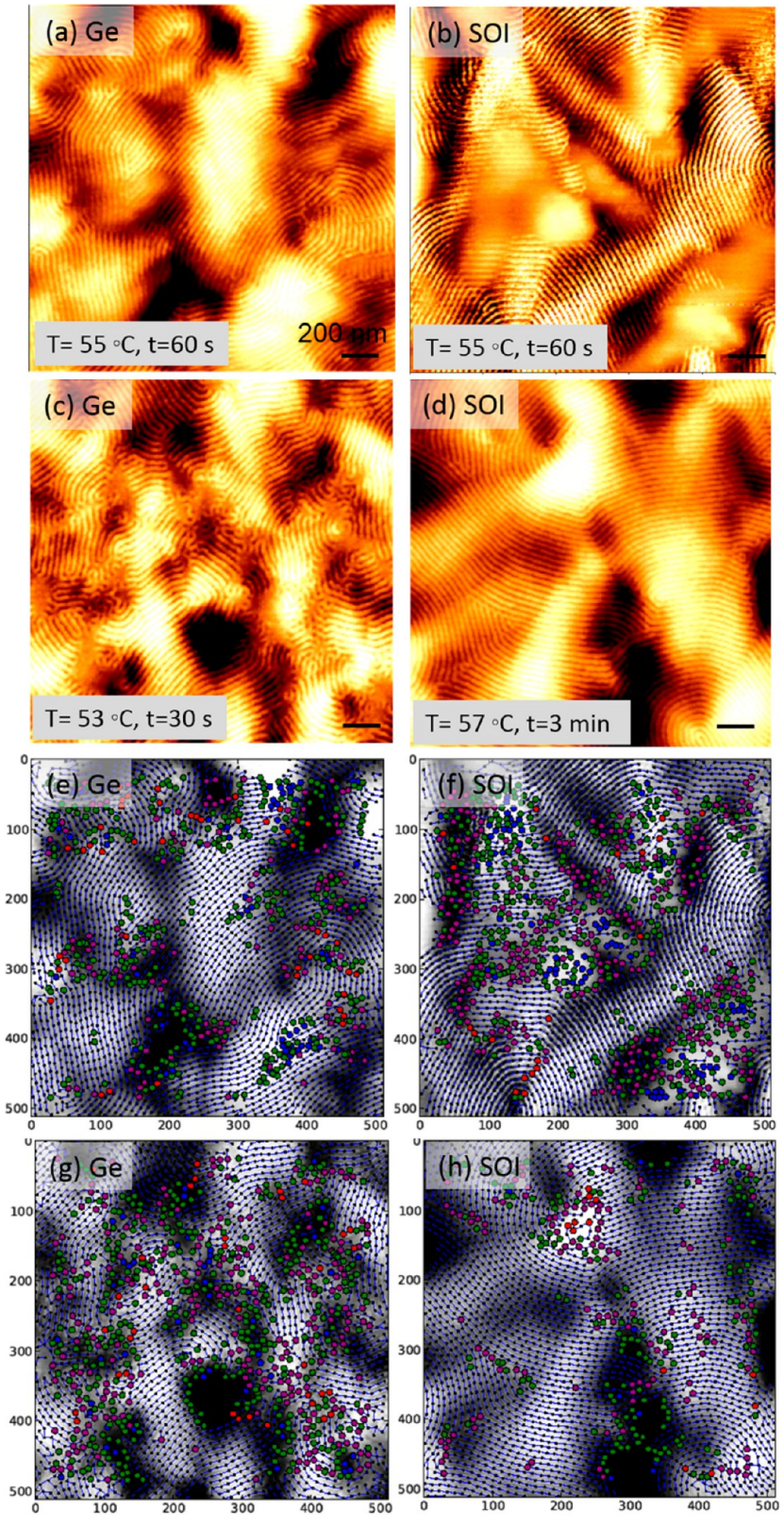

Figure 6. AFM topography images of solvo-microwave annealing of the PS-*b*-PLA film on different substrates: (a) 60 s at 55 °C and (c) 30 s at 53 °C on Ge and (b) 60 s at 55 °C and (d) 180 s at 57 °C on SOI substrate. The scale bars are 200 nm. (e–h) Defect analysis output. The average line length is longer on (f) SOI (1430 nm) than on (h) Ge (1750 nm). Also see Figure 9.

2c (1370 nm) is higher than that in Figure 2a (1303 nm) and Figure 2b (829 nm). The defect density (Figure 9b) is also lower in the sample annealed at a higher temperature (Figure 2c). However, annealing temperatures of 58 °C and above lead to the dewetting of the film. We believe that the saturation vapor pressure of the solvent during annealing has a profound effect. The vapor pressure of THF can be calculated using the Antoine equation (eq 2). *A*, *B*, and *C* are Antoine constants,

dx.doi.org/10.1021/la503137q | *Langmuir* 2014, 30, 10728–10739

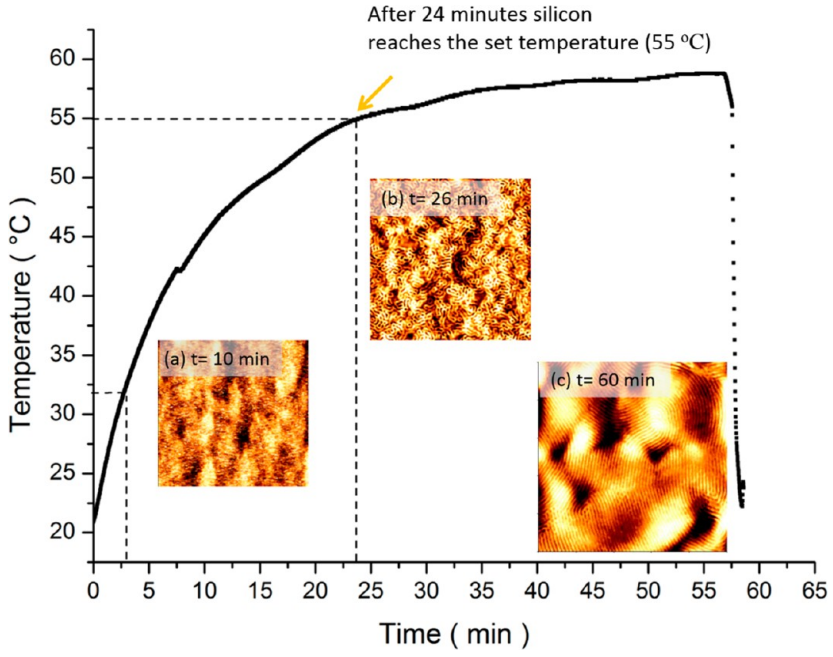

Figure 7. In situ temperature measurement of the silicon substrate during solvent annealing in the oven at 55 °C and with THF. Inset (a) is an AFM topography image of the PS-*b*-PLA film after 10 min of annealing, which shows no microphase separation, and inset (b) is after 26 min (2 min after Si reached 55 °C). Inset (c) is after 60 min of annealing. All AFM topography images are 2 × 2 μm^2.

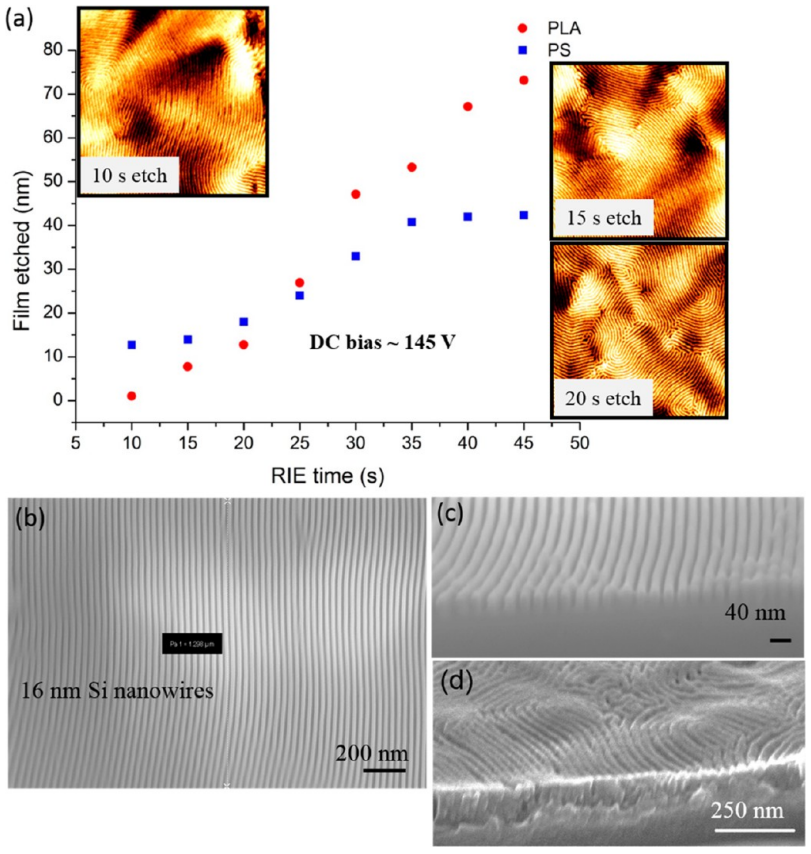

Figure 8. Etch rate of PS and PLA homopolymers in RIE at a dc bias of 145 V. (a) Initially PLA has a slower etch rate due to the high-sputtering-yield C═O group, but after 20 a when the C═O bond is broken, PLA is etched faster than PS. The insets in (a) are the topographic AFM images of PS-*b*-PLA after 10, 15, and 20 s etch times. Silicon nanowires (16 nm) fabricated by using PS-*b*-PLA as a template after 60 s of solvo-microwave annealing with THF and a 25 s RIE etch, followed by RIE-ICP pattern transfer. (b) Top-down SEM image of Si nanowires and (c) SEM cross section of (b). (d) SEM cross section of the stained sample after solvo-microwave annealing and prior to PLA removal.[30]

dx.doi.org/10.1021/la503137q | *Langmuir* 2014, 30, 10728−10739

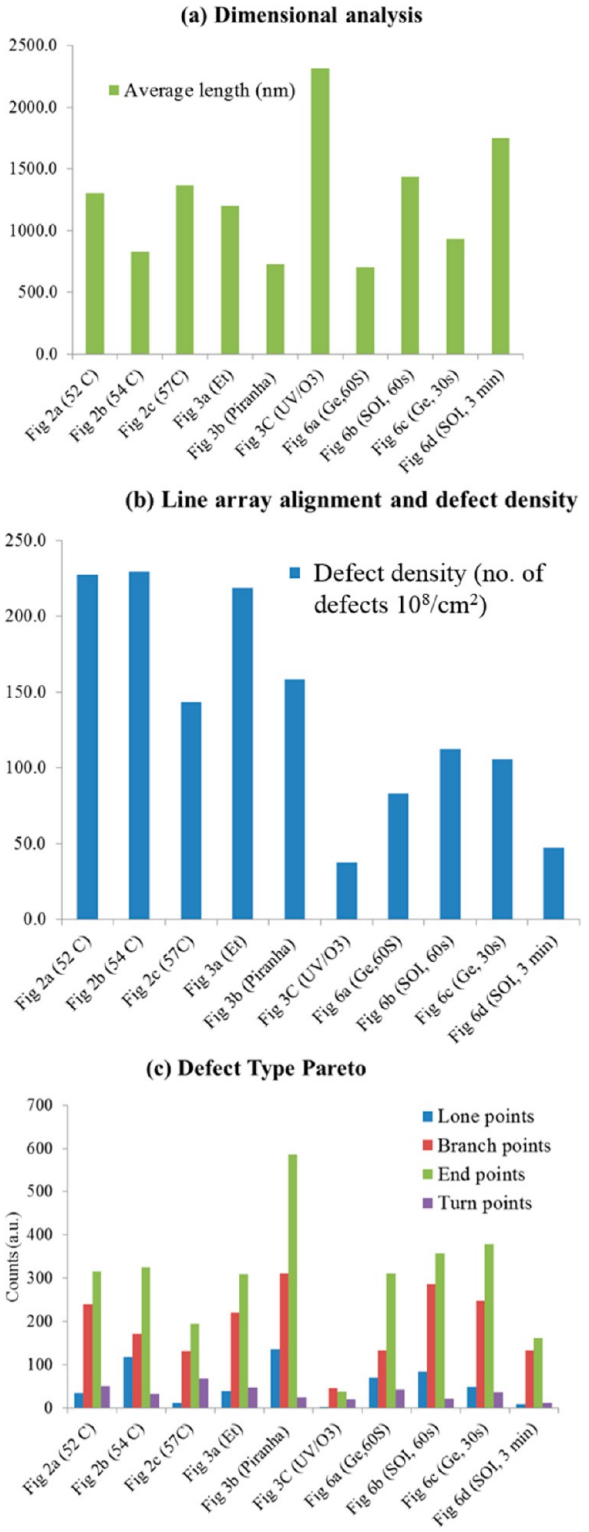

Figure 9. Quantitative defect analysis of images in Figures 2, 3, and 6. (a) Average line length (nm), (b) defect density, and (c) color-coded defect types.

and for 23 < T < 100 °C, A = 6.99, B = 1202.29, and C = 226.254 (which gives the vapor pressure in mmHg).[32] THF has a vapor pressure of 19.8 kPa at room temperature. Increasing the temperature to above 58 °C raises the vapor pressure to 78 kPa, and at this higher pressure, cooling and removing the sample from the vial leads to condensation and dewetting.

$$P = 10^{A-[B/(C+T)]} \quad (2)$$

Choice of Solvent for Solvo-Microwave Annealing. It was observed that the choice of solvent in solvo-microwave annealing follows similar rules to conventional solvent annealing, i.e., a neutral solvent for both blocks is required with the added need for solvent molecule polarity in microwave annealing. We examined different annealing solvents including chloroform, acetone, toluene, tetrahydrofuran (THF), water, and mixtures thereof. Table 1 shows the properties of the solvents and their affinities for PS and PLA. Apart from THF, none of the above-mentioned solvents led to observable microphase separation. Acetone is a polar solvent and PLA-selective, while chloroform is nonpolar and PS-selective.[16] Annealing PS-*b*-PLA with either acetone or chloroform did not induce lateral microphase separation. The affinity of one block with the solvent, for example, PLA with acetone, will encourage the migration of PLA to the surface to shield the PS chains from unfavorable contact with a nonsolvent.[16] THF, however, is a polar solvent and selective for both PS and PLA. As there is no strong preference of the blocks for the solvent, the polymer/air surface will be neutral for both components. This provides an equal opportunity for either block to be present on the polymer/air interface, and this will lead to lateral microphase separation. The polar property of THF is the major advantage during microwave annealing. As a polar substance, THF can absorb microwave energy and heat up very fast, which could subsequently lead to a fast self-assembly route in PS-*b*-PLA films. This is discussed in more detail below in the in situ temperature measurement experiment.

Table 1. Affinity of PS and PLA for Different Solvents[16,33]

solvent	$\chi_{PS\text{-}solvent}$	$\chi_{PLA\text{-}solvent}$	selectivity	polarity
acetone	1.30	0.28	PLA selective	polar
chloroform	0.34	<0.5	PS selective	nonpolar
chlorobenzene	1.01	1.21	PS selective	polar
THF	0.15	0.62	neutral but slightly more selective for PS	polar

The surface energies of PS and PLA are very close ($\gamma^{PS} \approx$ 40.7 mJ/m^2 and $\gamma^{PLA} \approx$ 38.3 mJ/m^2).[34] The neutrality of the silicon surface for PS and PLA and also the neutrality of the polymer/air surface for both blocks when exposed to THF provide an ideal condition for the perpendicular alignment of the domains on the Si substrate, provided that χN > 10.5. The Flory–Huggins interaction parameter (χ) between PS and PLA at a given temperature (T) can be calculated using eq 3 as reported by Zalusky et al.:[8]

$$\chi(T) = \frac{98.1}{T} - 0.112 \quad (3)$$

The degree of polymerization for our PS-*b*-PLA system is calculated as N = 418.6. Under our experimental conditions, i.e., $T \approx$ 55 °C, the phase segregation strength χN is about 78 in the upper limit of the intermediate- segregation regime.[35] To improve the long-range order and also the overall coverage of the samples, we cleaned the silicon substrate with ethanol and piranha solution and also cleaned the silicon substrates by exposing the sample to UV/ozone for 45 min prior to casting. The samples were then microwave annealed at 55 °C with THF. Figure 3 demonstrates the results following surface modification. A perpendicular alignment of lamellar domains was observed for all substrates. However, the best patterns were

dx.doi.org/10.1021/la503137q | Langmuir 2014, 30, 10728–10739

achieved through UV/ozone treatment (Figure 3b). The pattern has a pitch of 34 nm. Defect analysis in Figure 9a shows that the (UV/ozone)-treated sample has an average line length of 2319 nm, i.e., 3 times longer than the piranha-cleaned substrate (725 nm). With this knowledge, further experiments on silicon and alternative substrates were carried out after cleaning the substrate via exposure to UV/ozone treatment.

In Situ Temperature Measurement of Si and the Polymer Film during Microwave Annealing. Microwaves are electromagnetic waves that are absorbed by polar materials with an electronegativity greater than 0.5.[36] When a polar material is exposed to microwave radiation, the molecules try to align themselves with respect to the alternating electromagnetic field. These oscillations are resisted by other intermolecular forces, and work done by the alternating electric field in overcoming these resistive forces manifests itself as heat.[37−39] There are three possibilities accountable for enhancing the reaction rate in the microwave-assisted process:[37,38] (1) the thermal (kinetic) effect, which means that high temperature is achieved rapidly due to microwave absorbance of the polar materials, (2) specific thermal microwave interaction caused by the unique nature of microwave dielectric heating, and (3) the microwave-specific nonthermal interaction. (See Table 2 in ref 40 for more details.) Silicon is transparent to electromagnetic radiation. However, impurity and dopants in silicon can lead to microwave absorption to some extent. Hung and Gliessman[41] were the first to observe impurity conduction in semiconductors. Soon after, the ac impurity conduction in silicon was measured in the microwave frequency range.[42] The concentration of impurity and whether an ac or dc current is applied can affect the microwave absorption in silicon. To understand the interaction of microwave with different components in our experiment, i.e., substrates, polymers, and solvents, we have carried out an in situ temperature measurement of silicon by attaching an external temperature probe to the back of the substrate and monitoring the temperature of silicon directly via the external sensor during exposure to microwave irradiation. Figure 4 shows the setup. More details can be found in the Experimental Section. We used p-type silicon with a 2 nm native oxide layer on top. The purpose of the experiment was to investigate if there is excessive heat rise in the silicon substrate during microwave irradiation, which leads to the fast assembly of block copolymers. The temperature of the polymer film was also monitored during microwave annealing. The result is shown in Figure 5. As seen in Figure 5a during microwave annealing in our experiment, the temperature of neither the silicon substrate nor the PS-*b*-PLA film rose above the set value of 55 °C. Indeed, the temperature of the silicon substrate was ∼20 °C less than the temperature of the glass vial, i.e., the control temperature of 55 °C. One assumes that the dopant level in our silicon substrate is not high enough for significant microwave absorption either through ionized impurity pairs or due to the hopping process.[43] In the Zhang and Buriak et al. work, it has been shown that the resistivity of the substrate can affect the defect density in the PS-*b*-P2VP film.[9] In the Borah et al. work,[11] it was suggested that the substrate plays a passive role. In the recently published work by Buriak et al.,[12] it is shown that the underlying silicon substrate is the key to the rapid heating observed. In our present study, it seems that the temperature rise through the heat transfer in the silicon substrate is not the major mechanism that results in the rapid self-assembly of PS-*b*-PLA films. In Figure 5a, the temperature of the film during microwave annealing of PS-*b*-PLA is less than 30 °C, well below the glass temperature of PLA (T_g = 49 °C). It appears that the high vapor pressure of THF and the consequent increase in polymer swelling are at least partially responsible for the fast self-assembly of the PS-*b*-PLA system. THF is a polar molecule that rapidly absorbs microwave radiation. As discussed above, the vapor pressure of THF at 55 °C is 3.5 times higher than at room temperature. The polymer network responds to the significant osmotic pressure built up in a short time on top of the film. The swollen and stretched polymer chains will release the osmotic pressure by letting the solvent vapor diffuse to the network of polymer chains, which most likely leads to the suppression of the glass-transition temperature of the film. We also cannot rule out the effect of having "hot" THF molecules present in the film leading to heating and free volume inclusion. In Figure 5b, the microwave power range during 2 min of microwave exposure is plotted. In an ideal experiment, the microwave power should be constant during the annealing time. However, with our microwave unit, it is possible to adjust the power only indirectly. The power is applied to reach the user-defined temperature.

Mechanism of Microwave-Assisted Self-Assembly. To obtain deeper insight into the underlying mechanism of self-assembly during microwave energy, we studied the PS-*b*-PLA films on different substrates, i.e., silicon, germanium, and silicon on an insulator (SOI). In a recently published work by Buriak and coworkers,[12] the heating of the substrate is considered the primary source of heating and microphase separation. However, they were observed in the absence of solvent, and the temperature is much higher than our experimental condition (∼200 °C). The effect of the substrate during microwave irradiation can be studied from two different points of view: kinetics and thermodynamics. Our in situ temperature measurement (Figure 5) showed that the temperature of silicon does not rise dramatically during solvo-microwave annealing, and yet rapid microphase separation occurs within 60 s (Figure 3). Although the possibility of direct microwave heating of the substrate seems to be a minor component of solvo-microwave annealing, it was considered worthwhile to investigate the effect of the substrate on the kinetics of pattern formation during microwave annealing. Thus, we repeated the experiment on a germanium substrate, which has a higher dielectric constant (k = 16) than silicon (k = 12) and SOI (silicon on an insulator with a 140 nm buried oxide layer). If the substrate employed for microwave irradiation experiments is the primary basis for inducing fast kinetics, then it should take longer for the PS-*b*-PLA film to microphase separate on germanium than on silicon as it takes longer to heat up because of its higher dielectric constant. However, despite this assumption our result shows that in fact microphase separation of the PS-*b*-PLA film can happen almost twice as fast on germanium than on silicon and also at a slightly lower temperature (Figure 6c). These results emphasize the significant contributing influence of solvent vapor that acts as a plasticizer for rapid BCP self-assembly regardless of the substrate used. However, by comparing the PS-*b*-PLA films on both silicon and germanium substrates at 55 °C for 60 s (Figures 3c and 6a), one can observe that the coherence length is longer on silicon than on germanium. Figure 9a provides statistical data on the average length of features. We expected to see a similar trend for an SOI substrate, but as shown in the topographic AFM image in Figure 6d, the annealing time on the SOI substrate is noticeably longer than on silicon. Only 60 s

dx.doi.org/10.1021/la503137q | *Langmuir* 2014, 30, 10728−10739

of annealing at 55 °C for SOI leads to PS-*b*-PLA self-assembly. However, to achieve a long-range-order pattern similar to that observed on silicon (Figure 3c), PS-*b*-PLA films on SOI required 3 min of solvo-microwave annealing. This is perhaps due to the existence of the buried oxide layer (140 nm thick) in the substrate that increases the resistivity of the substrate. The following question arises: if the resistivity of the substrate plays a significant role in kinetics of microphase separation during solvo-microwave annealing (observed from comparing the results for silicon with SOI), then why does it take a shorter experimental treatment for the self-assembly of the film on germanium, which has a higher dielectric constant than silicon? To obtain more insight into the role of the substrate, we carried out an in situ temperature measurement on the PS-*b*-PLA film on silicon in the oven. The conditions were similar to the experiment in the microwave. The film was put inside an enclosed glass jar with 2−5 μL THF next to it at 55 °C. A thermometer was attached at the back of the substrate, and the temperature of the silicon was monitored. As shown in the graph in Figure 7, the temperature of silicon rises immediately after putting the sample in the oven, and it reaches 32 °C (similar to the silicon temperature in the microwave) in less than 3 min. Comparing the microwave-annealed film in Figure 3c with the film annealed in the oven (inset a in Figure 7), in both samples the temperature of the substrate is 32 °C, but the former sample shows microphase separation while there is no lateral microphase separation for the sample in the oven even after 10 min. Evidently, this is linked to THF, which has not reached the threshold vapor pressure of 70 kPa at 55 °C as described earlier. It takes 24 min for silicon to reach the set temperature of 55 °C. After reaching 55 °C, we kept the sample in the oven for another 2 min (similar to the microwave annealing condition) and then removed the sample after 26 min of solvent annealing. As shown in inset b in Figure 7, a microphase-separated pattern forms. This is because the vapor pressure of THF has reached a minimum threshold to induce microphase separation of the PS-*b*-PLA BCP. However, after one compares the microphase-separated pattern obtained with microwave annealing (Figure 3c) to solvent annealing in the oven (Figure 7b), it is obvious that the former has much better long-range order. Keeping the sample in the oven for long enough (about an hour) results in much improved long-range order (inset c in Figure 7). This is due to the different mechanism of heating in the oven in comparison to heating in the microwave because it takes longer for THF to reach the critical pressure. During solvo-microwave annealing, THF, which is a polar solvent, absorbs microwave energy once exposed to microwave irradiation. This leads to a rapid increase in the solvent vapor pressure in a very short time. Subsequent diffusion of the solvent vapor through the voids and free volume in the polymer network swells and mobilizes the polymer chains and contributes to fast self-assembly of the film. In the oven, however, THF heats up through a different mechanism. The heating in the oven is through convection and conduction; therefore, it takes longer for THF to reach and build up a suitable pressure (nominal pressure: 70 kPa at 55 °C) to trigger swift microphase separation in the PS-*b*-PLA film. In normal annealing in the oven, the solvent molecules have a thermal energy profile, i.e., vibration; however, in the microwave they are electronically and rotationally excited and have high-energy states besides thermal. During microwave annealing, some very high energy states can be created. These additional energies pass into the polymer, causing efficient local heating.

The comparison of the solvo-microwave annealing process in the microwave and the oven confirms that in our case study PS-*b*-PLA system, fast self-assembly is a kinetic effect primarily governed by the solvent vapor pressure. Although the role of the substrate cannot be ruled out, it seems the substrate plays a secondary role in this case. We speculate that there might be a threshold for the temperature of the substrate for fast self-assembly. Furthermore, characteristics of the native oxide such as roughness and crystallographic orientation could have an impact. However, these possible influential factors are the subject of future work. Nevertheless, the chemistry between the substrate and the polymers affects the degree of the order in the pattern and the uniformity of the film shown in Figure 6.

Etch and Pattern Transfer. In order to show that the perpendicular lamella patterns traverse the entire film and the technique could be applied for generation of silicon circuit elements, a successful recipe was developed for partial removal of PLA using a dry etch procedure performed in an Oxford Instruments Plasmatech in RIE mode using a mixture of Ar/O_2 gas. We also tried different wet etch processes. The comparison of the methods and a detailed etch study of PS-*b*-PLA is published separately[30] and will not be presented here. Prior to being etched, the PS domains were stained with RuO_4 to increase the contrast for SEM imaging. Figure 8d is the cross-sectional SEM image of the PS-*b*-PLA film after solvo-microwave annealing. The perpendicular domains of PS and PLA span the entire film thickness (~200 nm), suggesting that the morphology is consistent throughout the film. It has been shown that the etch rate of polymers is related to the sputtering factor.[44] Since carbon has a small sputtering yield, the etching of the carbon will be the slowest and hence the rate-determining step. The etch rate is inversely proportional to the number of carbon atoms. However, the number of oxygen atoms in a monomer enhances the etch rate according to the Ohnishi parameter determined from eq 4[44]

$$\nu \propto \frac{N}{N_C - N_O} \tag{4}$$

where ν is the etch rate, N is the total number of atoms in a monomer unit, and N_C and N_O are the numbers of carbon and oxygen atoms in a monomer unit. Using eq 4, the etch rate of PS (C_8H_8) and PLA ($C_3H_6O_3$) can be calculated. However, as the number of carbon and oxygen in PLA are the same, the etch rate of PLA cannot be calculated theoretically. We determined the etch rate of PS and PLA experimentally. (More details can be found in ref 30.) The etch rate of the PS and PLA homopolymer is compared in Figure 8. One can see that the etch rate of PS is higher initially, but after 20 s of etching, the PLA removal rate is faster. Comparing the insets (topographic AFM images) in Figure 8a, it seems that the etch is not one-dimensional and removes the polymer laterally as well. The higher etch rate of PLA is correlated to a greater number of oxygen atoms in the monomer. However, PLA contains C═O groups in its chain. C═O groups have much a higher sputtering yield than carbon (there is no oxygen atom in PS chain). The C═O group in PLA is responsible for the initial slower etch rate compared to that for PS. However, at longer etch times when the C═O bond is broken, the PLA etch rate accelerates. Figure 8b shows the top-down and SEM cross-sectional images of the film after the etch and pattern transfer. The remaining PS mask after the PLA etch was pattern

dx.doi.org/10.1021/la503137q | *Langmuir* 2014, 30, 10728−10739

transferred to a silicon substrate using a SF_6/C_4F_8 etch[3] followed by a thermal oxidation step to remove all traces of polymer. The silicon nanowires shown in Figure 8c are 16 nm wide and 45 nm high.

Defect Analysis. The defect analysis obtained from the method described earlier[15] enabled us to estimate the defect density, making it possible to statistically quantify the order of the line patterns within the experimental error on the basis of the density of turn points in the line array. Figure 9 summarizes the statistics for the samples studied here. From Figure 9a,b, it is clear that (UV/ozone)-treated silicon (Figure 3c) has the highest average line length and lowest defect density. Untreated silicon substrates (Figure 2a−c) have a high level of defects as illustrated in the data in Figure 9. Note that the analyzed area might be different for different images. The analyzed area is given in pixel by pixel dimensions, and we use the scale of the image to convert it into cm^2 as this is the common unit for industry. As a result of this conversion, a sample that has a higher total number of defects (e.g., in Figure 9c) might have a lower defect density in Figure 9b. Therefore, for comparison purposes Figure 9c provides more overall information about the samples. According to our estimation, the analysis uncertainty rise due to the variety in image magnification is found to be below 5%.

CONCLUSIONS

We have demonstrated the fast self-assembly of a high-χ, lamellar PS-*b*-PLA thin film utilizing microwave irradiation in the presence of THF for 60 s. A quantitative defect study shows that UV/ozone treatment of a silicon substrate prior to spin casting improves the long-range order dramatically. To probe the route of fast self-assembly of PS-*b*-PLA during solvo-microwave annealing, we carried out an in situ temperature measurement of silicon and the polymer film by attaching an external thermometer to the back of the substrate and on top of the film, recording their temperatures separately. Our results show the temperature of silicon and PS-*b*-PLA does not rise excessively during solvo-microwave annealing. Considering that Si and SiO_2 are not polar, they do not absorb microwave energy. Therefore, the heat transfer happens through conduction and convection rather than microwave absorption. With the range of temperature we applied (less than 60 °C), although the temperature of silicon rises rapidly, it is not high enough (~32 °C) to lead to fast self-assembly in such a short period of time. We suggest that polar THF that absorbs electromagnetic radiation in the microwave range plays a major role in the rapid self-assembly process observed. The nominal vapor pressure of THF increases from 19.8 kPa at room temperature to 70 kPa at 55 °C within seconds of microwave exposure. The high vapor pressure of THF in a sealed vessel provides fast access for diffusion to the depth of the film, which gives the chains enough mobility to microphase separate into well-ordered domains. Comparing the in situ temperature measurement of silicon in the microwave and in the oven confirms our theory that the substrate plays a less-important role during solvo-microwave annealing in comparison to the use of solvent. In the oven, silicon reached a temperature of 32 °C in less than 3 min, and no microphase separation was observed, whereas during solvo-microwave annealing, while the silicon reaches the same temperature, a long-range-order pattern forms. The reason is that in the oven at 32 °C, the vapor pressure of THF is not high enough to make the film swell sufficiently during that period of time. During solvo-microwave annealing, however, some very high energy states can be created as polar THF absorbs microwave energy very fast. These additional energies can pass into the polymer, causing efficient local heating which leads to the fast self-assembly effect.

Leaving the film in the oven for longer time, we observe a microphase-separated pattern, but it is poorer than the pattern obtained by microwave. This suggests that kinetics, i.e., the rate of film swelling and diffusion, affects the order and the coherence length of the pattern. Nevertheless, there might be a threshold for the temperature of the substrate to initiate self-assembly. Solvo-microwave annealing of a PS-*b*-PLA film on a germanium substrate which has a higher dielectric constant than silicon but takes a shorter time than silicon confirms the key role of THF as the primary cause of rapid self-assembly. However, a longer annealing time was required for an SOI substrate that has a thicker buried oxide layer and thus a higher dielectric constant than silicon. The longer annealing time needed for SOI substrates suggests that a possible minimum substrate temperature is required for effective pattern formation of block copolymers during solvo-microwave annealing. We measured the etch rate of PS and PLA homopolymers experimentally. PLA is etched faster due to the presence of oxygen in the back chain. Following an RIE-ICP etch, a successful pattern transfer led to the fabrication of 16 nm silicon nanowires. Our process provides a simple and effective means of pattern formation for an on-chip etch mask.

AUTHOR INFORMATION

Corresponding Author

*E-mail: p.mokarian@ucc.ie.

Present Address

(S.R.) Department of Micro and Nanotechnology, Technical University of Denmark.

Author Contributions

The manuscript was written through the contributions of all authors. All authors have given approval to the final version of the manuscript.

Notes

The authors declare no competing financial interest.

ACKNOWLEDGMENTS

We gratefully acknowledge Science Foundation Ireland (SFI) CSET/CRANN and a LAMAND NMP FP7 grant for funding this project. We thank Peter Gleeson and Matthew Shaw, staff of Intel and the AML (Advanced Microscopy Laboratory) in CRANN, for assistance with microscopy.

REFERENCES

(1) Herr, D. J. C. Directed Block Copolymer Self-assembly for Nanoelectronics Fabrication. *J. Mater. Res.* **2011**, *26*, 122−139.

(2) Farrell, R. A.; Petkov, N.; Shaw, M. T.; Djara, V.; Holmes, J. D.; Morris, M. A. Monitoring PMMA Elimination by Reactive Ion Etching from a Lamellar PS-b-PMMA Thin Film by ex Situ TEM Methods. *Macromolecules* **2010**, *43*, 8651−8655.

(3) Borah, D.; Shaw, M. T.; Rasappa, S.; Farrell, R. A.; O'Mahony, C.; Faulkner, C. M.; Bosea, M.; Gleeson, P.; Holmes, J. D.; Morris, M. A. Plasma Etch Technologies for the Development of Ultra-Small Feature Size Transistor Devices. *J. Phys. D: Appl. Phys.* **2011**, *44*, 12.

(4) Takahashi, H.; Laachi, N.; Delaney, K. T.; Hur, S. M.; Weinheimer, C. J.; Shykind, D.; Fredrickson, G. H. Defectivity in Laterally Confined Lamella-Forming Diblock Copolymers: Thermodynamic and Kinetic Aspects. *Macromolecules* **2012**, *45*, 6253−6265.

(5) Chang, S.-W.; Vogel, E. E.; Ginzburg, V. V.; Murray, D. J.; Kramer, J. W.; Weinhold, J. D.; Chuang, V. P. W.; Sharma, R.; Evans, J. P.; Landes, B.; Ge, S.; Trefonas, P.; Hustad, P. D. Designing New Materials and Processes for Directed Self-Assembly Applications. *Proc. SPIE 8323, Alternative Lithographic Technologies IV*, San Jose, CA, March 26, 2013, Vol. *8680*, doi: 10.1117/12.2011604.
(6) Lodge, T. P.; Dalvi, M. C. Mechanisms of Chain Diffusion in Lamellar Block Copolymers. *Phys. Rev. Lett.* **1995**, *75*, 657−660.
(7) Yokoyama, H. Diffusion of Block Copolymers. *Mater. Sci. Eng. R* **2006**, *53*, 199−248.
(8) Zalusky, A. S.; Olayo-Valles, R.; Wolf, J. H.; Hillmyer, M. A. Ordered Nanoporous Polymers from Polystyrene-Polylactide Block Copolymers. *J. Am. Chem. Soc.* **2002**, *124*, 12761−12773.
(9) Zhang, X. J.; Harns, K. D.; Wu, N. L. Y.; Murphy, J. N.; Buriak, J. M. Fast Assembly of Ordered Block Copolymer Nanostructures through Microwave Annealing. *ACS Nano* **2010**, *4*, 7021−7029.
(10) Zhang, X. J.; Murphy, J. N.; Wu, N. L. Y.; Harris, K. D.; Buriak, J. M. Rapid Assembly of Nano lines with Precisely Controlled Spacing from Binary Blends of Block Copolymers. *Macromolecules* **2011**, *44*, 9752−9757.
(11) Borah, D.; Senthamaraikannan, R.; Rasappa, S.; Kosmala, B.; Holmes, J. D.; Morris, M. A. Swift Nanopattern Formation of PS-b-PMMA and PS-b-PDMS Block Copolymer Films Using a Microwave Assisted Technique. *ACS Nano* **2013**, *7*, 6583−96.
(12) Jin, C.; Murphy, J. N.; Harris, K. D.; Buriak, J. M. Deconvoluting The Mechanism of Microwave Annealing of Block Copolymer Thin Films. *ACS Nano* **2014**, *8*, 3979−91.
(13) Borah, D.; Shaw, M. T.; Holmes, J. D.; Morris, M. A. Sub-10 nm Feature Size PS-b-PDMS Block Copolymer Structures Fabricated by a Microwave-Assisted Solvothermal Process. *ACS Appl. Mater. Interfaces* **2013**, *5*, 2004−2012.
(14) Higuchi, T.; Shimomura, M.; Yabu, H. Reorientation of Microphase-Separated Structures in Water-Suspended Block Copolymer Nanoparticles through Microwave Annealing. *Macromolecules* **2013**, *46*, 4064−4068.
(15) Simão, C. T. D.; Khunsin, W.; Amann, A.; Morris, M. A.; Sotomayor Torres, C. M. In Defect Analysis and Alignment Quantification of Line Arrays Prepared by Directed Self-assembly of a Block Copolymer. *SPIE Proc.* **2014**, *9050*, 905028.
(16) Vayer, M.; Hillmyer, M. A.; Dirany, M.; Thevenin, G.; Erre, R.; Sinturel, C. Perpendicular Orientation of Cylindrical Domains Upon Solvent Annealing Thin Films of Polystyrene-b-Polylactide. *Thin Solid Films* **2010**, *518*, 3710−3715.
(17) Olayo-Valles, R.; Guo, S. W.; Lund, M. S.; Leighton, C.; Hillmyer, M. A. Perpendicular domain orientation in thin films of polystyrene - Polylactide diblock copolymers. *Macromolecules* **2005**, *38*, 10101−10108.
(18) Baruth, A.; Rodwogin, M. D.; Shankar, A.; Erickson, M. J.; Hillmyer, M. A.; Leighton, C. Non-lift-off Block Copolymer Lithography of 25 nm Magnetic Nanodot Arrays. *ACS Appl. Mater. Interfaces* **2011**, *3*, 3472−3481.
(19) Guo, S. W.; Rzayev, J.; Bailey, T. S.; Zalusky, A. S.; Olayo-Valles, R.; Hillmyer, M. A. Nanopore And Nanobushing Arrays from ABC Triblock Thin Films Containing Two Etchable Blocks. *Chem. Mater.* **2006**, *18*, 1719−1721.
(20) Sinturel, C.; Vayer, M.; Morris, M.; Hillmyer, M. A. Solvent Vapor Annealing of Block Polymer Thin Films. *Macromolecules* **2013**, *46*, 5399−5415.
(21) Han, W.; Byun, M.; Zhao, L.; Rzayev, J.; Lin, Z. Q. Controlled Evaporative Self-Assembly of Hierarchically Structured Bottlebrush Block Copolymer with Nanochannels. *J. Mater. Chem.* **2011**, *21*, 14248−14253.
(22) Han-Hao Cheng, I. K.; Yu, A.; Chuang, Y.; Blakey, I.; Jack, K. S.; Whittaker, A. K. EUVL compatible, LER solutions using functional block copolymers, *Proc. SPIE, Alternative Lithographic Technologies IV*, March 1, 2012, San Jose, CA; Vol. *8323*, doi: 10.1117/12.916744.
(23) Keen, I.; Yu, A. G.; Cheng, H. H.; Jack, K. S.; Nicholson, T. M.; Whittaker, A. K.; Blakey, I. Control of the Orientation of Symmetric Poly(styrene)-block-poly(D,L-lactide) Block Copolymers Using Statistical Copolymers of Dissimilar Composition. *Langmuir* **2012**, *28*, 15876−15888.
(24) Lo, K.-H.; Chen, M.-C.; Ho, R.-M.; Sung, H.-W. Pore-Filling Nanoporous Templates from Degradable Block Copolymers for Nanoscale Drug Delivery. *ACS Nano* **2009**, *3*, 2660−2666.
(25) Chen, D. J.; Gong, Y. M.; He, T. B.; Zhang, F. J. Effect of crystallization on the lamellar orientation in thin films of symmetric poly(styrene)-b-poly(L-lactide) diblock copolymer. *Macromolecules* **2006**, *39*, 4101−4107.
(26) Welander, A. M.; Kang, H. M.; Stuen, K. O.; Solak, H. H.; Muller, M.; de Pablo, J. J.; Nealey, P. F. Rapid Directed Assembly of Block Copolymer Films at Elevated Temperatures. *Macromolecules* **2008**, *41*, 2759−2761.
(27) Kim, S. O.; Solak, H. H.; Stoykovich, M. P.; Ferrier, N. J.; de Pablo, J. J.; Nealey, P. F. Epitaxial Self-assembly of Block Copolymers on Lithographically Defined Nanopatterned Substrates. *Nature* **2003**, *424*, 411−414.
(28) Mokarian-Tabari, P.; Collins, T. W.; Holmes, J. D.; Morris, M. A. Brushless and Controlled Microphase Separation of Lamellar Polystyrene-b-Polyethylene Oxide Thin Films for Block Copolymer Nanolithography. *J. Polym. Sci., Part B: Polym. Phys.* **2012**, *50*, 904−909.
(29) Rice, R. H.; Mokarian-Tabari, P.; King, W. P.; Szoszkiewicz, R. Local Thermomechanical Analysis of a Microphase-Separated Thin Lamellar PS-b-PEO Film. *Langmuir* **2012**, *28*, 13503−13511.
(30) Cummins, C.; Mokarian-Tabari, P.; Holmes, J. D.; Morris, M. A., Selective Etching of Polylactic Acid in Poly(styrene)-block-poly(D,L)lactide Diblock Copolymer for Nanoscale Patterning. *J. Appl. Polym. Sci.* **2014**, *131*.
(31) Haubruge, H. G.; Jonas, A. M.; Legras, R. Staining of Poly(Ethylene Terephthalate) by Ruthenium Tetroxide. *Polymer* **2003**, *44*, 3229−3234.
(32) Wichterle, I.; Linek, J. *Antoine Vapor Pressure Constants of Pure Compounds*; Academia, 1971
(33) Ho, R. M.; Tseng, W. H.; Fan, H. W.; Chiang, Y. W.; Lin, C. C.; Ko, B. T.; Huang, B. H. Solvent-Induced Microdomain Orientation in Polystyrene-b-Poly (L-Lactide) Diblock Copolymer Thin Films for Nanopatterning. *Polymer* **2005**, *46*, 9362−9377.
(34) Ringardlefebvre, C.; Baszkin, A. Behavior of Poly(D,L-lactic acid) Monolayers at the Air-water-interface- Effect of Spreading Solvents. *Langmuir* **1994**, *10*, 2376−2381.
(35) Matsen, M. W.; Bates, F. S. Unifying Weak- and Strong-Segregation Block Copolymer Theories. *Macromolecules* **1996**, *29*, 1091−1098.
(36) Pauling, L. *The Nature of the Chemical Bond and the Structure of Molecules and Crystals: An Introduction to Modern Structural Chemistry*, 3rd ed.; Cornell University Press: Ithaca, NY, 1960.
(37) Galema, S. A. Microwave Chemistry. *Chem. Soc. Rev.* **1997**, *26*, 233−238.
(38) Gabriel, C.; Gabriel, S.; Grant, E. H.; Halstead, B. S. J.; Mingos, D. M. P. Dielectric Parameters Relevant to Microwave Dielectric Heating. *Chem. Soc. Rev.* **1998**, *27*, 213−223.
(39) Mingos, D. M. P.; Baghurst, D. R. Applications of Microwave Dielectric Heating Effects to Synthetic Problems in Chemistry. *Chem. Soc. Rev.* **1991**, *20*, 1−47.
(40) Jacob, J.; Chia, L. H. L.; Boey, F. Y. C. Thermal and Non-Thermal Interaction of Microwave Radiation with Materials. *J. Mater. Sci.* **1995**, *30*, 5321−5327.
(41) Hung, C. G. JR Resistivity and Hall Effect of Germanium at Low Temperatures. *Phys. Rev.* **1954**, *96*, 1226−1236.
(42) Tanaka, S.; Fan, H. Y. Impurity Conduction in P-Type Silicon at Microwave Frequencies. *Phys. Rev.* **1963**, *132*, 1516−1526.
(43) Tanaka, S.; Hanamura, E.; Kobayashi, M.; Uchinoku, K. Microwave Absorption in Silicon at Low Temperatures. *Phys. Rev. A* **1964**, *134*, A256−A264.
(44) Gokan, H.; Esho, S.; Ohnishi, Y. Dry Etch Resistance of Organic Materials. *J. Electrochem. Soc.* **1983**, *130*, 143−146.